Cereal Research Communications 43(3), pp. 426–437 (2015)
DOI: 10.1556/0806.43.2015.3.8

Sensitive Detection of Aflatoxin B1 Molecules on Gold SPR Chip Surface Using Functionalized Gold Nanoparticles

A. Majzik[1], V. Hornok[1], D. Sebők[1], T. Bartók[3], L. Szente[4], K. Tuza[4] and I. Dékány[1,2]*

[1]MTA-SZTE Supramolecular and Nanostructured Materials Research Group, University of Szeged, Dóm tér 8, H-6720 Szeged, Hungary
[2]Department of Medical Chemistry, Faculty of Medicine, University of Szeged, Dóm tér 8, H-6720 Szeged, Hungary
[3]Faculty of Engineering, University of Szeged, Moszkvai krt. 5–7, H-6725 Szeged, Hungary
[4]CycloLab Ltd, Illatos út 7, H-1097 Budapest, Hungary

(Received 24 January 2015; 15 April 2015;
Communicated by A. Goyal)

Due to the warm and favourably humid climate of Southern Hungary, the maize is one of the most important crops. The protection against crop damage caused by fusarium and Aspergillus species is essential. Detection of aflatoxin B1 (AFB1) molecules in cereal crops by selective sensors is important, while they can cause serious diseases in humans and animals if they enter the food chain. Our main objective was to develop selective AFB1 sensor with increased sensitivity applying βCD-functionalized gold nanoparticles (AuβCD NPs) in surface plasmon resonance (SPR) measuring apparatus. The nanoparticles ca. 10 nm in diameter were prepared in the presence of thiol-modified cyclodextrin. The adsorption isotherms of AFB1 on bare, thiol-modified cyclodextrin and AuβCD NPs covered Au film surface were calculated using SPR platform. The AFB1 concentration can be quantitatively determined in the 0.001–23.68 ng/mL range. The AuβCD NPs were found to be highly sensitive and exhibited a remarkably low limit of detection (*LOD*; 1 pg/mL) without using other analytical reagents.

Keywords: aflatoxin, gold nanoparticles, cyclodextrin, biosensor, SPR

Introduction

The protection against maize crop damage caused by fusarium and Aspergillus species is essential in the agriculture. Aflatoxins are carcinogenic and harmful for gene and occur in nature. The aflatoxin B1 molecule is the most efficient impurity in food (Pestka et al. 1980). It is very useful to develop new and more sensitive methods for quantitative determination of hydrophobic molecules (Du et al. 2007; Kham et al. 2007; Pál et al. 2009; Varga et al. 2009). Although numerous procedures can detect and determine the aflatoxin derivatives, the most typical one is the time-delayed analysis of aflatoxin derivatives by thin-layer chromatography, high-performance liquid chromatography, overpressured-layer chromatography, and enzyme-linked immunosorbent assay (Li and Zhang 2009;

* Corresponding author; E-mail: i.dekany@chem.u-szeged.hu; Phone: +36-62-544-210; Fax: +36-62-544-042

Manetta et al. 2005; Moricz et al. 2007; Peiwu et al. 2009; Urusov et al. 2014b; Var et al. 2007). The detection of mycotoxins by SPR from food-stuff has already been reported in several publications and those with low molecular weight (aflatoxin, ochratoxin A) were determined by SPR immunosensors (Daly et al. 2000; Hodnik and Anderluh 2009; Homola 2008; Li et al. 2012; Yuan et al. 2009). The guest molecules (AFB1) interact with the cavity of the host molecule with non-covalent forces (Szejtli 2004).

Gold nanoparticles AuNPs have attracted significant attention in novel electronic and optical devices for detection of biomolecules and drugs in various biomedical applications due to their non-toxic nature and excellent biological compatibility (Huang et al. 2006; Perez-Juste et al. 2005; Sharma et al. 2010; Turkevich 1985). The surface functionalization of gold can be performed with thiol-modified cyclodextrin (βCD-$(SH)_2$). The CDs are cyclic oligosaccharides, where glucose molecules are linked by glycosidic bonds to form a cylindrical structure. The cylinder forms a truncated cone, which has a hydrophilic rim and a lipophilic interior. Due to this specific structure, CD possesses an ability to form host–guest inclusion complexes with a wide range of compounds, thus increasing the water solubility of hydrophobic compounds (Mandal et al. 2010; Szejtli 1995). Aflatoxin derivatives can be bound to the internal rings of βCD-$(SH)^2$ molecules. The βCD-$(SH)_2$ molecule can be attached to gold surfaces by covalent bond (Ogoshi and Harada 2008).

Our study was focused on the adsorption of AFB1 on βCD-$(SH)_2$ functionalized gold surface (AuβCD NPs) using UV-Vis spectroscopy and SPR technique. The aim of this work was to devise a very sensitive detection method for AFB1 on AuβCD NPs comprising of using SPR analytical experiments. We aimed to study the effect of βCD functionalization of the AuNPs and also to study the AFB1 inclusion into the βCD rings. The application of βCD ensures the selective binding into the rings, the extremely sensitive optical response of AuNPs can enhance the sensitivity. This direct method thus is suitable for determination of AFB1 in important alimentary target compounds by functionalized AuNPs. An additional advantage is that no additional reagents are needed for the analysis as compared to previous studies (Daly et al. 2000; Dunne et al. 2005; Moon et al. 2012).

Materials and Methods

Materials

For the preparation of βCD-$(SH)_2$ modified AuNPs, sodium-borohydride ($NaBH_4$) (Sigma-Aldrich) reducing agent was used in aqueous $HAuCl_4 \cdot 3H_2O$ solution (PubChem CID: 28133) (Sigma-Aldrich) in presence of βCD-$(SH)_2$ (produced by Cyclolab Ltd., Hungary) (Kim et al. 2008). The 5 mL of $HAuCl_4$ precursor solution (0.8 mg/mL) was added to 5 mL 0.6 mg/mL βCD-$(SH)_2$ solution and the mixture was stirred for 10 min and afforded the AuNPs by addition of 10 mL 0.2 mM ice cold $NaBH_4$ (PubChem CID: 22959485) (the ratio of AuNPs and $NaBH_4$ was 10:1). The aqueous AuβCD NP dispersion was stirred vigorously at room temperature overnight. The molar ratio was

βCD-$(SH)_2$: Au = 1:8. The concentration of the functionalized AuNPs with βCD-$(SH)_2$ was 0.197 mg/ml. In all cases the dispersions were prepared in MQ ultrapure water.

AFB1 standard (PubChem CID: 186907) was used (produced by Fluka, RM, ≥99%, 2 μg/ml in acetonitrile) in the experiments. The acetonitrile content was 0.3% in every experiment (the volume ratio of H_2O/acetonitrile was 99.7/0.3, *v/v*).

Methods

The UV-Vis spectra of AuNPs were recorded in Shimadzu UV-1800 spectrophotometer in the λ = 200–800 nm range using a 1 cm quartz cuvette.

The average particle diameter of AuNPs was determined by high-resolution transmission electron microscope (HR-TEM, FEI Tecnai G^2 (200 kV)).

Zeta potential data were obtained with a Horiba Nano Particle Analyzer SZ-100. The measurements were recorded at 25 ± 0.1 °C.

A two-channel SPR sensor platform developed at the Institute of Photonics and Electronics (Prague) was applied. The SPR measurements were performed on a thin gold layer (50 nm thickness) film deposited on a glass substrate produced by the above mentioned company. When the incoming light is reflected on the interface of about 50 nm thick metal layer through a prism, at a certain angle of incidence in total internal reflection, the characteristic light absorption (attenuation of reflected light) can be observed. This is the Surface Plasmon Resonance phenomena. It is very sensitive to the change of reflective index of the media, i.e. molecular adsorption to the metal interface in the evanescent light distance, and monitoring the change allows high-sensitivity measurement of molecular-adsorption movement on surface. The sensitivity of the SPR apparatus is 54,000 nm/RIU (refractive index unit) and the resolution is $<10^{-7}$ RIU. The temperature was kept at 20 °C and flow rate was 20 μL × min^{-1}. Volumes of 500 ml of all samples were measured in all cases. The streaming medium was MQ water for desorption between samples. The recorded spectra were analyzed by a special software that allows determination of the resonant wavelength in both sensing channel. Adsorption isotherms were determined for the measured molecules/AuNPs. Each adsorption step for increasing concentration was followed by desorption in water stream and only the remaining adsorbed amounts are presented on the adsorption isotherms. The adsorbed mass (m^s) was calculated from the measured Δλ values at given concentration. After calibration, the Δλ values can be converted to surface concentration expressed in "number of moles" of adsorbed species per surface area (Γ in nmol/cm^2). In our dilute solutions according to J. Homola et al., at the Au plasmon maximum of 710 nm a wavelength shift of 1 nm corresponds to a change in adsorbed mass of 26.3 ng/cm^2 (Homola 2008). In our experiments *dn/dc* = 0.14 mL/mg (*dn/dc* is the dependency of refractive index on concentration of adsorbent in the solution; typically 0.1–0.3 mL/mg) (Ho et al. 2005; Liedberg and Lundström 1993; Tumolo et al. 2004). The monolayer coverage was determined from the linear form of the Langmuir isotherm:

$$\frac{1}{\Gamma} = \frac{1}{\Gamma_m} + \frac{1}{K \cdot c} \quad (1)$$

where Γ denotes surface excess concentration of adsorbed species per surface area, Γ_m in pmol/cm^2 monolayer surface concentration and K is the equilibrium constant (Feijter et al. 1978; Sebők et al. 2013). Marvin was used for drawing, displaying and characterizing chemical structures, substructures and reactions (ChemAxon 2013). The geometrical calculated cross-sectional area of AFB1 molecule is 0.82 nm^2 using the Marvin-Sketch theoretical model calculation method. From this and the Γ_m data the calculated theoretical adsorbed monolayer capacity can be determined for AFB1. Comparing the experimental and the calculated data, the theoretical surface coverage can be calculated.

Every sample contained the above-mentioned 0.3% acetonitrile content in aqueous solutions. The isotherms were corrected by the change in Δλ caused by the acetonitrile. Three parallel measurements were carried out on SPR platform and the average standard deviation (sd) of the results were smaller than ±4%. Adsorption of the following molecules and systems were measured by SPR on Au film (these conventions are used in Table 1):

Table 1. The values determined for different systems from SPR measurements and calculated from the Langmuir equation

	Measured systems by SPR	$\Delta\lambda_{max}$, nm	m^s_m, ng/cm^2	m^s, ng/cm^2 at measured max. concentration	$1/\Gamma_m$, cm^2/pmol	Γ_m, pmol/cm^2
i)*	AFB1 on Au film	0.19	5.67	5.00	0.055	18.18
ii)*	βCD-(SH)$_2$ on Au film	0.34	9.25	8.94	0.131	7.65
iii)*	AFB1 in βCD-(SH)$_2$ rings	0.42	14.45	11.05	0.021	46.30
iv)*	AuβCD NPs on Au film	3.30	51.28	86.79	0.019**	51.28***
v)*	AFB1 on AuβCD NPs surface on Au film	0.53	15.61	13.94	0.020	50.00

*The symbols used in the methods section.
**Expressed in mass units ($1/m^S_m$, cm^2/ng AuβCD).
***Expressed in mass units (m^S_m, ng AuβCD NP/cm^2).

i) AFB1 molecules
ii) βCD-(SH)$_2$ molecules
iii) AFB1 molecules by inclusion in βCD-(SH)$_2$ rings
iv) AuβCD
v) incorporation of AFB1 molecules in βCD-(SH)$_2$ rings attached to AuNPs (AuβCD nanodispersion)

Results

AFB1 adsorption on SPR platform

SPR measurements were carried out in order to determine the adsorbed amounts of AFB1 and βCD-$(SH)_2$ on Au thin film. Series of AFB1 solutions (0.17–33.5 ng/mL) were introduced to the SPR gold film and the amount of physically adsorbed AFB1 increases with the concentration in all cases (Fig. 1). The maximal adsorbed amount of AFB1 – remaining bound to the surface after washing with MQ water – equals to 5.00 ng/cm^2 (Fig. 1), which value was calculated on the basis of equation 1, the linear representation of the adsorption isotherm.

The Γ_m (monolayer surface concentration) was calculated from the experimental data for AFB1 as apparent value: Γ_m = 18.18 pmol/cm^2. The monolayer adsorbed mass of AFB1 molecules on SPR chip surface (m^s_m = 5.67 ng/cm^2) is very small, because a large proportion of the AFB1 molecules eliminates from the surface upon washing for 15 minutes and only the physically adsorbed AFB1 remains on the Au film. The geometrical calculated cross-sectional area of AFB1 molecule is 0.82 nm^2 using the Marvin-Sketch theoretical model calculation method and the calculated theoretical adsorbed monolayer capacity for AFB1 is 202.5 pmol/cm^2. Comparing the experimental and the calculated data, the theoretical surface coverage is: 18.18/202.5 = 8.98%. The results are summarized in Table 1**.**

βCD-$(SH)_2$ adsorption on SPR platform

The adsorbed amount of βCD-$(SH)_2$ molecules on Au film was determined by SPR technique. The concentration of βCD-$(SH)_2$ was gradually increased up to 35 ng/mL. In the 5–35 ng/mL concentration range 8.94 ng/cm^2 was adsorbed on the Au film. In a hexagonal close-packed structure, the cross sectional area of βCD-$(SH)_2$ calculated by Marvin-Sketch is 2.30 nm^2. After the desorption process the remaining apparent adsorbed amount of βCD-$(SH)_2$ was found to be Γ_m = 7.65 pmol/cm^2 for "monolayer" adsorption capacity and the apparent adsorbed amount was m^s_m = 9.25 ng/cm^2 calculated from the Langmuir

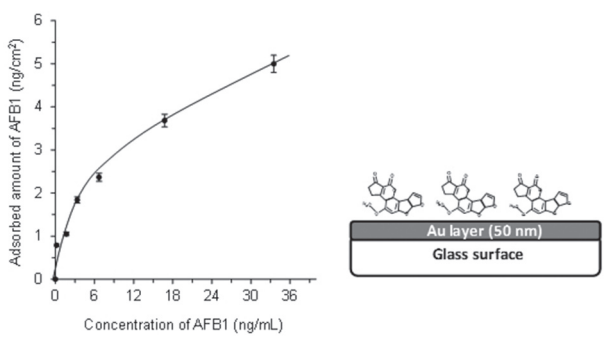

Figure 1. Adsorption isotherm of AFB1 aqueous solution on Au film and the schematic representation of AFB1 molecules adsorbed on Au surface

isotherm (see Table 1). During the βCD-$(SH)_2$ adsorption onto the SPR Au film surface the chemically adsorbed molecules were not eliminated from the surface with washing after desorption period. Theoretical adsorbed monolayer capacity for βCD-$(SH)_2$ was 72.2 pmol/cm^2. Comparing the experimental and the calculated data, the theoretical surface *coverage* is 7.65/72.2 = 10.6%. After the analysis of the adsorption data we can conclude that only 9–10% of the pristine Au film is coated at the above mentioned quasi equilibrium adsorption/desorption process in a flow system for surface sensing of the investigated analyte molecules.

AFB1 inclusion in βCD-$(SH)_2$ rings on SPR Au film

Prior to the adsorption of AFB1 molecules on SPR Au film, the gold surface was functionalized with 35 ng/mL of βCD-$(SH)_2$ solution. AFB1 solutions (0.11–23.68 ng/mL) were introduced in the flow cell of SPR platform after the adsorption equilibrium (Fig. 2). On the βCD-$(SH)_2$-modified Au film, the surface concentration was obtained to be 46.30 pmol/cm^2. Enhanced adsorbed amount of AFB1 was reached by applying βCD molecules, while 11.05 ng/cm^2 on βCD-modified SPR surface was (Fig. 2) about 200% more than in the case of AFB1 without βCD on the Au film.

Characterization of βCD-$(SH)_2$ functionalized AuNPs

The AuβCD nanodispersion with 0.197 mg/mL concentration was produced by the above described method. Cyclodextrin molecules attach, via their thiol groups, to the surface of the AuNPs being formed in the course of reduction (Fig. 3). The maximal wavelength of plasmon band characteristic of spherical AuNPs was observed at λ = 539 nm when the aureate anions were reduced in presence of βCD-$(SH)_2$ molecules, while the plasmon maximum is apparent at λ = 519 nm reduced by $NaBH_4$ without cyclodextrin due to the surface functionalization. The plasmon resonance maximum of AuβCD nanodispersion is shifted by 9–11 nm towards higher wavelengths by the addition of various amounts (3–33 ng/mL) of AFB1 (Fig. 3). The cavities of cyclodextrin molecules contain polar water

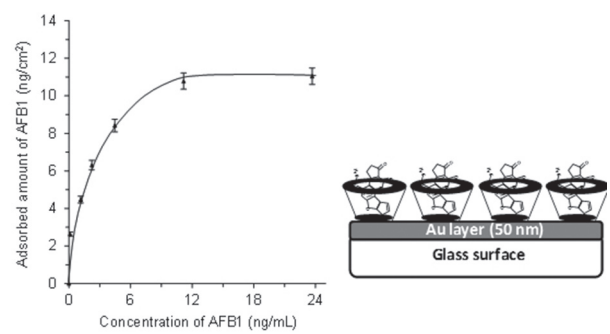

Figure 2. Adsorption isotherm of AFB1 on βCD-$(SH)_2$ modified Au film measured on SPR platform and schematic representation of incorporated AFB1 in βCD-$(SH)_2$ molecules on Au film

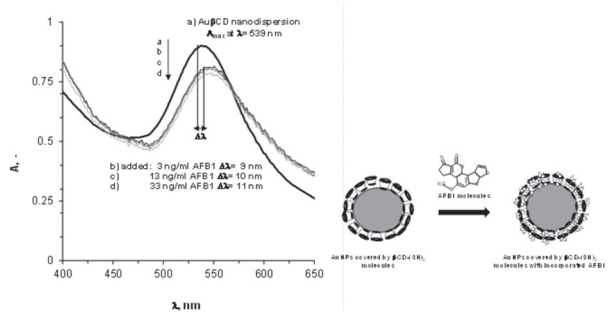

Figure 3. Absorbance spectra of AuβCD nanodispersions added AFB1 and schematic presentation of AuNPs covered by βCD-$(SH)_2$ before and after incorporation of AFB1 molecules

molecules, which are easily exchanged for less polar components such as the apolar AFB1 molecule. The shift of the plasmon resonance maxima towards higher wavelengths indicates linkage of the coated particles present. The zeta potential of the AuβCD NPs nanodispersion increased from –28 mV to –41 mV as the effect of AFB1 addition, but remains the same value by further increase in AFB1 concentration. It can be established that, by binding of thiolated cyclodextrins on AuNPs and the further inclusion of AFB1 leads to the formation of more stable gold nanodispersion as concluded from the ζ-potential values.

Adsorption of AuβCD NPs on SPR platform

The adsorption of the AuβCD NPs on Au film was also examined. The AuβCD NP dispersions were added with increasing concentration (in range 0.81–9.96 ng/mL) in a flow system on the SPR platform. The Au film surface was first saturated at 5.0 ng/mL concentration of AuβCD NPs; when further AuβCD NPs was added, the increasing adsorbed amount indicated the development of additional layers. At 9.96 ng/mL concentration of the AuβCD NPs, a maximal amount of 86.8 ng/cm^2 is attached to the Au film. The surface concentration was obtained to be 51.28 pmol/cm^2.

AFB1 inclusion in AuβCD NPs on SPR platform

A sample of the freshly prepared AuβCD NPs nanodispersion (with 3.7 ng/mL gold content) was added to the Au film. This selected concentration saturated the SPR chip surface in monolayer. Then the AFB1 standard solution was introduced with 0.11–23.68 ng/mL concentrations and again followed by washing with MQ water among the addition of every concentration step (Fig. 4).

The absorbed quantities in the function of the concentration are presented in Fig 4. In case the AuβCD NPs are attached to the surface of the Au film, plasmonic coupling takes place on the surface between the Au film and the AuβCD NPs, since – according to the Kretschmann measuring setup – in this case the spreading plasmons excited within the Au

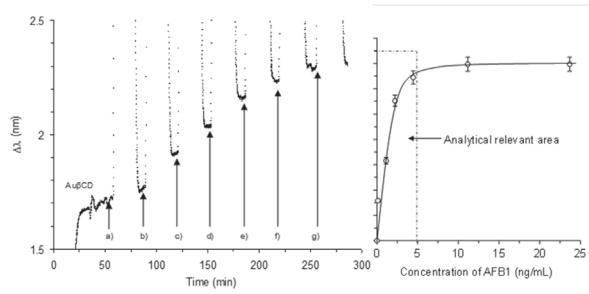

Figure 4. SPR curve of AFB1 (b) 1, c) 5, d) 10, e) 30, f) 60 pg/ml) on a) AuβCD NPs modified surface measured on SPR platform, and adsorption isotherm of AFB1 on AuβCD NP-modified Au film measured on SPR platform

film are coupled with the localized plasmons (LSPR) of the AuNPs (Daly et al. 2000). Figure 4 shows that AFB1 adsorbed preferentially on the βCD-modified AuNP surface, the adsorption capacity is ~30% more than on βCD-$(SH)_2$ surface, i.e. 13.94 ng/cm^2 AFB1 adsorbed irreversibly on the AuβCD-modified surface. The area occupied by an adsorbed molecule and the relative monolayer surface concentration of the AFB1 molecules on the AuβCD-modified surface in the above listed systems are found in Table 1. The highest coverage of AFB1 achievable on AuβCD-covered layers was 2.5–2.75 fold larger than adsorbed amount on the surface covered only by βCD-$(SH)_2$.

Adsorption of AFB1 standard solution for characterization of the sensitivity was measured in the 1–60 pg/mL concentration range. When different amounts of AFB1 solution are added, sections corresponding to adsorption events are observed. Steeply decreasing desorption branches are seen at the last three concentrations (10–30 and 60 pg/mL), followed by baseline establishment at 2.26 nm (which is equal to 51.00 ng/cm^2). The amount of AFB1 adsorbed on the modified surface is calculated by subtracting the baseline value from the value obtained for AuβCD. The calculation of AFB1 concentration was carried out on the basis of Δλ values measured by SPR platform. After fitting a fourth-degree polynomial to the first section of the isotherm in Fig. 5, the concentration of AFB1 can be calculated from the polynomial equation, if the wavelength shift (Δλ) of the AFB1 solution is known and its concentration falls into this range. As clearly seen on the SPR curve, even an AFB1 concentration of 1 pg/mL can be measured, because the Δλ = 0.19 nm is well detectable with this technique.

Discussion

Several methods are known for the selective detection of aflatoxin B1 molecule. Some research groups focus on the rapid and simple detection from maize grift samples. The usual methods in AFB1 detection include HPLC, immunoassay and SPR methods (Daly et al. 2000; Li and Zhang 2009; Moricz et al. 2007). Urusov et al. (2014a) describe a sensitive method for the immunochromatographic determination of aflatoxin B1. The aptamer assay used by Shim et al. (2014) exhibited a limit of detection of 0.11 ng/mL in

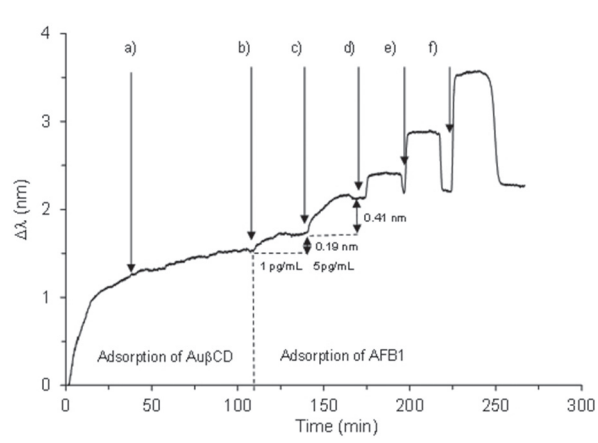

Figure 5. SPR curve of AFB1 (b) 1, c) 5, d) 10, e) 30, f) 60 pg/mL) on a) AuβCD NPs modified surface measured on SPR platform (acetonitrile content was ~2 ppm in every sample)

the 0.1 to 10 ng/mL concentration range. Some research groups also apply nanoparticles but without functionalization, thus the selectivity is less (Luan et al. 2015; Wang et al. 2014). An aptamer based assay working with fluorescence quenching of CdTe qantum dots was evaluated by Lu et al. (2015). The obtained LOD value was 1.4 nM with the advantage that this simple method may be extended to the analysis of other mycotoxins. Urusov et al. (2014b) also used AuNPs but without βCD and determined the limit of detection to 160 pg/mL if detected visually, and to 30 pg/mL via instrumental detection. This is significantly lower than the LOD of 2 ng/mL achieved by conventional lateral flow analysis using the same reagents. In contrast, there is no detectable signal below ~400 pg/mL using HPLC/APPI-MS techniques. The sensitivity of the AFB1 ELISA Kit is ~30 pg/mL.

Our method does not require expensive kit assay and also the SPR methodology is cheaper with at least 20% of the MS-HPLC techniques. As it turns out from the measurements, the functionalized AuNPs increase the sensitivity, resulting in a 200-fold improvement on the detection limit of AFB1. The disadvantage of this method is that the host–guest interaction is between AFB1 and cyclodextrin does not provide enough discrimination for a complex sample, although a preliminary cleaning of samples by gel-filtration chromatography (immune purification column, for example from AflaStar™ R by Romer Labs®) can result clean, interference free measurable solution after elution processes. Control experiments were performed using immune columns, those results are presented here.

The sensitivity of this functionalized AuNPs is $\Delta\lambda$ ~0.5 nm/ng for AFB1. The LOD concentration for standard AFB1 in acetonitrile medium is 1 pg/mL (Fig. 5). The procedure can also serve for determination of the adsorbed amount of AFB1 having a close relation – in the knowledge of adsorption isotherms – between the concentration of analyte molecules for the quantitative analysis of AFB1. The limit of detection for standard

AFB1 was found to be 0.1 ng/mL in 0.11–2.22 ng/mL concentration range and the low qualification concentration (LOQ) was 0.3 ng/mL at signal-to-noise ratio 10:1 on AuβCD plasmonic sensor unit. The LOD value for standard AFB1 was significantly improved compared to literature values measured to be 0.8 pg/mL in the 1–60 pg/mL concentration range at the signal-to-noise ratio 3:1 on AuβCD NPs (Fig. 5) (Dunne et al. 2005; Soft Flow Hungary 2013).

The results verify the application of CD-modified AuNPs in sensing AFB1 with high sensibility. Our SPR detector extended with βCD inclusion complexes exceeded the former detection limits. The measured LOD was 400 pg/mL from HPLC, whereas the lowest determined amount was 170 pg/mL determined with SPR. Other research groups also determined the detection limit of AFB1 in different SPR systems (Biacore or Plasmon II) or in ELISA Kit/buffer (Var et al. 2007) or by SPR Biacore system (Dunne et al. 2005; Soft Flow Hungary). The SPR Biacore system 3000 was more sensitive than the Biacore 1000 type instrument with LOD values of 190 pg/mL against 3000 pg/mL, while our detection limit in acetonitrile (2 ppm) was 170 pg/mL without AuNPs. The obtained 0.8 pg/mL value using the AuβCD NPs is at least 50 times smaller relative to the smallest obtained 25 pg/mL limit values determined by Var et al. in 2007 (see the experimental data in Table 2).

Table 2. The LOD values found in literature and our measured values on SPR platform for AFB1 molecules

Sensor systems/detection matrix	Detection limit (pg/mL)	Measured range (pg/mL)	Reference
SPR Biacore 1000/buffer	3,000	3,000–98,000	[Dunne et al., 2005]
SPR Biacore 3000/buffer	190	190–24,000	[Soft Flow Hungary, 2013]
SPR Plasmon II/acetonitrile (0.03%)	170	170–33,500	Measured values/on SPR platform
SPR Plasmon II/acetonitrile (0.03%)	170	110–23,680	Measured values/in βCD-$(SH)_2$ rings
SPR Plasmon II/ acetonitrile (2 ppm)	0.8	10–23,680	Measured values/on AuβCD NPs functionalized SPR platform
HPLC/APPI-MS/acetonitrile (60%)	400	1–500	Measured values/maize meal
ELISA Kit/buffer	25	25–200	[Var et al., 2007]

Acknowledgements

This research was supported by the European Union and the State of Hungary, co-financed by the European Social Fund in the framework of TÁMOP 4.2.4. A/2-11-1-2012-0001 'National Excellence Program' and PIMFCS_H, ERANET_hu_09-1-2010-0033.

References

ChemAxon 2013. Marvin 6.0.0. http://www.chemaxon.com

Daly, S.J., Keating, G.J., Dillon, P.P., Manning, B.M., O'Kennedy, R., Lee, H.A., Morgan, M.R. 2000. Development of surface plasmon resonance-based immunoassay for aflatoxin B(1). Agric. Food Chem. **48**:5097–5104.

Du, Y., Luo, X.L., Xu, J.J., Chen, H.Y. 2007. A simple method to fabricate a chitosan-gold nps film and its application in glucose biosensor. Bioelectrochem. **70**:342–347.

Dunne, L., Daly, S., Baxter, A., Haughey, S., O'Kennedy, R. 2005. Surface plasmon resonance-based immunoassay for the detection of aflatoxin B1 using single-chain antibody fragments. Spectroscopy Letters **38**:229–245.

Feijter, J.A., Benjamins, J., Veer, F.A. 1978. Ellipsometry as a tool to study the adsorption behavior of synthetic and biopolymers at the air-water interface. Biopolymers **17**:1759–1772.

Ho, C., Robinson, A., Miller, D., Davis, M. 2005. Overview of sensors and needs for environmental monitoring. Sensors **5**:4–37.

Hodnik, V., Anderluh, G. 2009. Toxin detection by surface plasmon resonance. Sensors **9**:1339–1354.

Homola, J. 2008. Surface plasmon resonance sensors for detection of chemical and biological species. Chem. Review **108**:462–493.

Huang, X., El-Sayed, I. H., Qian, W., El-Sayed, M. A. 2006. Cancer cell imaging and photothermal therapy in the near-infrared region by using gold nanorods. JACS **128**:2115–2120.

Kham, K., Guerrouache, M., Carbonnier, B., Laterges, M., Perrot, H., Millot, M.C. 2007. Supramolecular interactions between b-cyclodextrin and hydrophobically end-capped poly(ethylene glycol)s: A quartz crystal microbalance study. J. Coll. Interf. Sci. **315**: 800–804.

Kim, J.H., Kim, K.S., Manesh, K.M., Santhosh, P., Gopalan, A.I., Lee, K.-P. 2008. Self-assembly directed synthesis of gold nanostructures. Colloids and Surfaces A **313–314**:612–616.

Li, P., Zhang, Q. 2009. Immunoassays for aflatoxins. Trends Analyt. Chem. **28**:1115–1126.

Li, Y., Liu, X., Lin, Z. 2012. Recent developments and applications of surface plasmon resonance biosensors for the detection of mycotoxins is foodsuffs. Food Chem. **132**:1549–1554.

Liedberg, B., Lundström, I. 1993. Principles of biosensing with an extended coupling matrix and surface plasmon resonance. Sensors and Actuators A **11**:63–72.

Lu, Z., Chen, X., Wand, Y., Zheng, X., Li, C.M. 2015. Aptamer based fluorescence recovery assay for aflatoxin B1 using a quencher system composed of quantum dots and graphene oxide. Microchimica Acta **182**:571–578.

Luan, Y.X., Chen, Z.B., Xie, G., Chen, J.Y., Lu, A.X., Li, C., Fu, H.L., Ma, Z.H., Wang, J.H. 2015. Rapid visual detection of aflatoxin B1 by label-free aptasensor using unmodified gold nanoparticles. J. of Nanoscience and Nanotechnology **15**:1357–1361.

Mandal, A.K., Das, D.K., Das, A.K., Sen Mojumdar, S., Bhattacharyya, K. 2010. Study of gamma-cyclodextrin host-guest complex and nanotube aggregate by fluorescence correlation spectroscopy. J. Phys. Chem. B **115**:10456–10461.

Manetta, A.C., Di Giuseppe, L., Giammarco, M., Fusaro, I., Simonella, A., Gramenzi, A. 2005. High-performance liquid chromatography with post-column derivatisation and fluorescence detection for sensitive determination of aflatoxin M1 in milk and cheese. J. Chromatography A. **1083**:219–222.

Moricz, A., Fater, Z., Otta, K.H., Tyihak, E., Mincsovics, E. 2007. Over pressured layer chromatographic determination of aflatoxin B1, B2, G1 and G2 in red paprika. Microch. J. **85**:140–144.

Moon, J., Kim, G., Lee, S. 2012. A gold nanoparticle and aflatoxin B1-BSA conjugates based lateral flow assay method for the analysis aflatoxin B1. Materials **5**:634–643.

Ogoshi, T., Harada, A. 2008. Chemical sensors based on cyclodextrin derivatives. Sensors **8**:4961–4982.

Pál, L., Dublecz, K., Weber, M., Balogh, K., Erdélyi, M., Szigeti, G., Mézes, M. 2009. Effect of combined treatment with aflatoxin B_1 and T-2 toxin and metabolites on some production traits and lipid peroxide status parameters of broiled chickens. Acta Veterinaria Hungarica **57**:75–84

Peiwu, L., Qi, Z., Wen, Z., Jinyang, Z., Xiaomei, C., Jun, J., Lihua, X., Daohong, Z. 2009. Development of a class-specific monoclonal antibody-based ELISA for aflatoxins in peanut. Food Chem. **115**:313–317.

Perez-Juste, J., Pastoriza-Santos, I., Liz-Marzan, L.M., Mulvaney, P. 2005. Gold nanorods: Synthesis, characterization and applications. Coordination Chem. Review **249**:1870–1901.

Pestka, J.J., Gaur, P.K., Chu, F.S. 1980. Quantitation of aflatoxin B1 and aflatoxin B1 antibody by an enzyme-linked immunosorbent microassay. Appl. Envir. Microb. **40**:1027–1031.

Sebők, D., Csapó, E., Preocanin, T., Bohus, G., Kallay, N., Dékány, I. 2013. Adsorption of ibuprofen and dopamine on functionalized gold using surface plasmon resonance spectroscopy at solid-liquid interface. Croatia Chemica Acta **86**:287–295.

Sharma, A., Matharu, Z., Sumana, G., Solanki, P.R., Kim, C.G., Malhotra, B.D. 2010. Antibody immobilized cysteamine functionalized-gold nanoparticles for aflatoxin detection. Thin Solid Films **519**:1213–1218.

Shim, W.-B., Mun, H., Joung, H.-A., Ofori, J.A., Chung, D.-H., Kim, M.-G. 2014. Chemoluminescence competitive aptamer assay for the detection of aflatoxin B1 in corn samples. Food Control **36**:30–35.

Soft Flow Hungary 2013. ELISA Kit for determination of total aflatoxin (B1, B2, G1, G2). Technical documentation 301013.

Szejtli, J. 1995. Selectivity/structure correlation in cyclodextrin chemistry. Supramolecular Chem. **6**:217–223.

Szejtli, J. 2004. Past, present, and future of cyclodextrin research. Pure and Appl. Chem. **76**:1825–1845.

Tumolo, T., Angnes, L., Baptista, M.S. 2004. Determination of the refractive index increment (dn/dc) of molecule and macromolecule solutions by surface plasmon resonance. Anal. Biochem. **333**:273–279.

Turkevich, J. 1985. Colloidal Gold. Part I. Gold Bulletin **18**:86–91.

Urusov, A.E., Zherdev, A.V., Dzantiev, B.B. 2014a. Use of gold nanopatricle-labeled secondary antibodies to improve the sensitivity of an immunochromatographic assay for aflatoxin. Microchim Acta **181**:1939–1946.

Urusov, A.E., Petrakova, A.V., Vozniak, M.V., Zherdev, A.V., Dzantiev, B.B. 2014b. Rapid immunoenzyme assay of aflatoxin B1 using magnetic nanoparticles. Sensors **14**:21843–21857.

Yuan, J., Deng, D., Lauren, D.R., Aguilar, M.I., Wu, Y. 2009. Surface plasmon resonance biosensor for the detection of ochratoxin A in cereals and beverages. Analytica Chimica Acta **656**:63–71.

Var, I., Kabak, B., Gok, F. 2007. Survey of aflatoxin B1 in helva, a traditional Turkish food, by TLC. Food Control **18**:59–62.

Varga, J., Frisvad, J.C., Samson, R.A. 2009. A reappraisal of fungi producing aflatoxins. World Mycotoxin J. **2**:263–277.

Wang, X., Niessner, R., Knopp, D. 2014. Magnetic bead-based colorimetric immunoassay for aflatoxin B1 using gold nanoparticles. Sensors **14**:21535–21548.